

1994

Space Fed Subarrays using a Displaced Feed

Robert J. Mailloux
Air Force Research Laboratory
Sensors Directorate
80 Scott Drive
Hanscom AFB, Massachusetts, 01731-2909
E-mail: robert.mailloux@hanscom.af.mil

Abstract: A multiple beam (transform) feed for a phase-scanned lens has the desirable property of forming subarrays for the insertion of time delays across the large aperture. However, at certain scan angles and particular frequencies the multiple beam feed can have a focus at its front face. This phenomenon can be unacceptable when transmit amplifiers are used at this location since it requires that all power be provided from a few or even a single feed port. This paper presents a procedure for defocusing the feed to avoid the large dynamic range problem and spread the required power among a larger fraction of feed elements.

1. Introduction

Space fed overlapped subarray systems are an appropriate array architecture for inserting time delay into very large phased array systems. For arrays scanned to wide scan angles (say 60°), time delays become necessary when the required fractional bandwidth $\Delta f/f_0$ is more than the array beamwidth (in radians). This paper addresses a recently uncovered difficulty with such systems, one that is of major consequence if transmit modules are used at the feed output ports.

Figures 1 through 5 illustrate the use of time delayed subarrays for large arrays with phase shifters at the array face. An array with phase shifters alone forms its beam at the angle θ whose sine is

$$u = \sin \theta = (f_0 / f) \sin \theta_0 \quad (1)$$

Where θ_0 is the beam peak at center frequency f_0 . If the array is large, and its beamwidth narrow, then there can be significant loss, called "squint loss", due to the beam moving off of the target direction at frequencies away from center frequency. Grouping elements into contiguous subarrays, as shown in Figure 1, can reduce this squint loss, but can incur the large quantization lobes shown in the

DISTRIBUTION STATEMENT A

Approved for Public Release
Distribution Unlimited

20030225 113

figure. Figures 2 and 3 suggest that synthesizing special pulse-like subarray patterns can suppress these quantization lobes while simultaneously reducing the squint loss. Figure 4 shows that a space fed array configuration can be used with a multiple beam (or transform) feed to produce the desired pulse shaped subarray patterns, and then superimposed to form low sidelobe radiated beams.

The geometry of Figure 4 is often called a dual transform network or overlapped subarray network. Its behavior is described in several texts^{1, 2, 3} as well as in numerous journal articles^{4, 5}. In all of the cited references, it is assumed that the array is a passive network, or active devices are placed at the element level. The objective lens is an equal path length-structure with a cylindrical back face, and a single focal point. The lens has phase shifters at its front face, and these are used to produce a progressive phase front that scans the beam of the lens to any desired angle (θ_0) with direction cosine $u_0 = \sin \theta_0$. For this reason the objective lens is referred to as a "phase-shift" lens.

The objective lens is illuminated by a feed array that is in turn connected to a "transform" network, an $M \times M$ multiple-beam network which might be a Butler Matrix, a focusing lens, or it could be a set of amplifiers and A/D converters followed by a digital beamformer that performs a DFT operation. Each of these produces a set of overlapping sinc-like illuminations, spaced a distance D_0 apart across the main lens that constitute a set of overlapped subarrays. Each subarray radiates a pulse shaped pattern with phase center at the peak of a sinc-function. When all of the subarrays are driven by time-delayed signals, the array forms a beam that radiates in a fixed direction throughout a bandwidth that is roughly proportional to the subarray beamwidth. Typically the achievable instantaneous fractional bandwidth is about two-thirds of the theoretical maximum value $(D_0/\lambda_0 \sin \theta_0)^{-1}$.

Figure 5 shows several possible locations for transmit/receive (T/R) modules and poses a critical question that can impact the utility of these systems. Since they are most often proposed for large space arrays, there may be tens or even hundreds of thousands of elements at surfaces "A" and "B" (in the two dimensional case). Despite obvious advantages of having one module per element, the cost of so many modules often precludes further consideration of this approach. Surface "D" is not an ideal location for T/R modules because of the loss in the multiple beam feed in addition to loss at the objective lens. Surface "C" appears to be an ideal compromise, being closer to the radiating lens than surface "D." However, the transform feed is usually placed with its output elements along a straight line through the focus of the objective lens, and this requires that the feed be a classic

multiple beam feed. At certain scan angles and frequencies this feed will have a focus at its front face. The large variation in current amplitudes makes the array output power vary significantly, with sometimes a single transmitter supplying all the power. This may be of little consequence if the whole network is fed by a single, high powered transmit source, but it causes significant difficulty when using modern solid state transmit modules. It is this feature, which could be described as a dynamic range issue, or also as an issue of net available power, that this work has sought to address.

2. The Dynamic Range Issue

As noted in the introduction, an obvious location for T/R modules is at the front of the feed array (Surface "C"), since this surface requires only a modest number of modules, and only suffers the added power loss due to signal passing through the objective lens/phase shifter combination. Unfortunately the signals at this surface undergo extreme levels of dynamic range. The most striking example is the transmit case, when all subarrays are excited with equal amplitude and off center frequency. One can show that on some i 'th feed element, the largest value of signal I_i occurs when

$$u_o = \frac{+i}{M \frac{D_o}{\lambda_o}} \left(\frac{K}{1-r} \right) \quad \text{for} \quad -\left(\frac{M-1}{2} \right) \leq i \leq \left(\frac{M-1}{2} \right) \quad (2)$$

for then $I_i = M$. The element indices i are taken as integers or half integers, according to equation 2, and centered about the array center. In the expression above, $K=1$ for an orthogonal beamforming feed (Butler Matrix) and $k=r$ for a time delay lens (Rotman). Figures 6A and 6B show the currents I_i at several of these critical angles for $M = 16$ and $D_0/\lambda_0 = 16$ and $r = f/f_0 = 0.975$. The critical angles are slightly different for the two beamformers as indicated on the figure and are in accordance with equation 2. The element index number $i = 5.5$ is the only one with signal for the orthogonal beam feed case (6A), but for the time delayed lens (6B) that element has the strongest signal, but others have small residual signals. Figures 7A and 7B show the signals at some elements $-6.5 \leq i \leq -0.5$ as a function of scan angle for and illustrate the repetitive nature of these peaks and zeros. The zeros are all coincident for the orthogonal feed case (Fig 7A) and occur at different values of u_0 for the time delayed lens case. (Fig 7B).

Apart from this illustration of the severe dynamic range and power distribution problem, the figures also show that the region of peak amplitude moves across the face of the feed as the scan angle u_0 is varied, with most intensity near the feed array center for small u_0 and toward either array edge for larger $|u_0|$. Figure 7C shows the number of feed elements with significant power as a function of scan angle. This illustrates that for most angles only one of 16 feed elements carries significant power.

These three figures (5,6 and 7) have described the case of uniform illumination which is often the case for a transmitting radar. The receive case, often using a low sidelobe illumination, has a smaller dynamic range at the front face of the feed.

3. Analysis of the Geometry

Figure 8 shows the basic configuration and several relevant geometries that are proposed as solution. Assuming that the objective lens has a cylindrical back face, and the feed elements are located at $(y, z) = (y_i, h)$, with reference to Figure 8A, then the distance from each i 'th element to some point on the lens at some angle ϕ is

$$\rho_i^2 = F^2 + h^2 + y_i^2 + 2Fh\cos\phi - 2Fy_i \sin\phi \quad (3)$$

Throughout this paper the above (near field) representation for distance will be used instead of any far field approximation, because of the short focal lengths considered. It will be assumed that the entire structure is enclosed in a parallel plane medium so the problem is reduced to two dimensions.

Assuming some excitation currents I_i at each i 'th feed element, the currents at the back face of the objective lens are:

$$A(n) = \sum_i I_i \frac{e^{-jk_0\rho_i}}{\sqrt{\rho_i}} \quad (4)$$

where the currents I_i are given by the sum over the M values of the input signals J_m . Each input signal J_m , applied to the input port of the multiple beam feed produces a series of currents $I_i(m)$ at the feed's output ports, with i and m integers or half integers as given below. These currents are each weighted by the weights $w_i(m)$ and summed to give the total

$$I_i = \sum_m w_i(m) I_i(m) \quad (5)$$

where $I_i(m) = J_m e^{-jK 2\pi \left(\frac{m}{M}\right)i}$ (6)

and $K = 1$ for an orthogonal beam network (Butler Matrix)

and $K = \frac{f}{f_o} = r$ for a time delay feed (Rotman Lens etc.)

for $-\left(\frac{M-1}{2}\right) \leq i \leq \left(\frac{M-1}{2}\right)$ and $-\left(\frac{M-1}{2}\right) \leq m \leq \left(\frac{M-1}{2}\right)$

For an N -element objective lens, the far field radiation is given:

$$f(u) = \sum_{n=-(N-1)/2}^{(N-1)/2} A(n) e^{\frac{j2\pi}{\lambda_0} (r \sin \theta - \sin \theta_0) n d_L} \quad (7)$$

where the $\sin \theta_0$ term is due to the phase shift that has been added to scan the beam to θ_0 .

Equation 4 gives the aperture distribution A_n at the back face of the lens corresponding to the total current I_i . This expression is used for all calculations of radiated fields. However, for the purpose of determining the subarray signals J_m , it is convenient to assume a far field approximation. For the m 'th subarray, the aperture distribution on the objective lens back face is approximately

$$A(n) \approx \sum_{-(M-1)/2}^{(M-1)/2} w_i(m) I_i(m) e^{j \frac{2\pi i}{\lambda} d_y \sin \phi_n} \quad (8)$$

where we have defined the angle ϕ_n such that the location of the n'th element on the lens back face is

$$y_n = nd_L = F \sin \phi_n \quad (9)$$

$$so \quad \sin \phi_n = \frac{nd_L}{F}$$

and the peaks of the $A(n)$ illumination for any given "m" are

$$\text{at} \quad \frac{2\pi i}{\lambda} d_y \sin \phi_m = +2\pi K \left(\frac{m}{M} \right) i$$

$$\text{and} \quad nd_L = K \left(\frac{m}{M} \right) \frac{F\lambda}{d_y} \quad (10)$$

The distance between any two such peaks is the distance between an m'th subarray and an (m+1)'st subarray peak, or:

$$D = KF \frac{\lambda}{d_y} \frac{1}{M} \quad (11)$$

At center frequency ($f=f_0$) this spacing is:

$$D_o = \frac{F}{M} \frac{\lambda_o}{d_y} \quad (12)$$

so $D = D_o$ for a time delay beamformer

and $D = D_o/r$ for an orthogonal beamformer – (Butler Matrix).

The signals J_m are chosen to provide time delay for each m'th subarray, but in addition they need to compensate for the phase shift already introduced across the array.

$$J_m = |J_m| e^{j \frac{2\pi}{\lambda_o} u_o m D_o (1-r)} \quad (13)$$

This set of subarray level input signals has constant phase at center frequency ($r=1$) and at frequencies away from center frequency it introduces a time delay term while subtracting out the phases at locations mD_0 in the main lens. While this compensates exactly for the time delayed beamformer (Rotman Lens) configuration, it introduces a small “squint” error for the orthogonal beam (Butler Matrix) feed, since those subarray centers are located at mD across the main lens and their location varies with frequency. This could be compensated for digitally, and replace D_0 by D_0/r in the above, but throughout this discussion the equation 13 above is used directly, and is found to be a good approximation.

These currents $I_i(m)$ radiate to form the desirable pulse-shaped subarray patterns for time delay insertion at the subarray level by time-delaying the signals J_m . The steep skirts of the subarray patterns serve to suppress any grating lobes due to the periodic quantization. Figure 2 shows a typical subarray pattern formed by this geometry, and the array pattern for a 256-element array with 8 tapered subarray weights.

4. Results using a Displaced Feed

Figure 8 shows the basic configuration and several relevant geometries that are proposed as solution. The essence of the solution proposed here is to move the multi-beam feed either further from the lens than the focal point by the distance h ($h>0$ for case of Figure 8B) or closer to the lens ($h<0$ for case of Figure 8C). The logic then is to replace the multiple beam feed network by some synthesized network that, on transmit, produces either an appropriate converging field (Figure 8B) or a diverging field (Figure 8C). This new network is synthesized on the basis of having good subarraying properties, like the network and lens it replaces. The synthesis was conducted using an iterative alternating projection technique. Figure 9 outlines the procedure that is begun using the complex weights A_n in the aperture that were produced by the original focal plane beamformer. The far-field radiated pattern amplitude is computed and projected onto the space between two boundary upper and lower “masks”, M_U and M_L . The phase is initially constrained to have the same distribution as the phase of the focal plane feed, but left unconstrained for later iterations. The resulting far field distribution is then

inverse transformed back to the main lens, where it is truncated. Finally this solution is inverted using the LMS fit to the front face of the feed at its new location. This solution again is transformed using the near field transform (equation 4) and the procedure repeated until converged. The examples shown in this paper are for the geometry of Figure 8C.

The intention is to synthesize a network that can be implemented via digital beamformer, and in fact the advantage of digital beamforming is that a different set of weights can be selected for each subarray, in order to optimize performance.

Figure 10 compares two subarray pattern amplitudes for the subarray with index $m=-5.5$. The synthesis produces a pattern that is similar to that of the focal plane beamformer, but slightly narrower, indicating a reduced bandwidth. Since this synthesis is done digitally, it is convenient to synthesize a different set of weights $w_i(m)$ for each subarray (m) .

Figure 11 compares the current on element number -5.5 (fourth from the left edge of the feed) for the focal plane beamformer with that of the synthesized beamformer for a uniformly illuminated array. Both feeds show that the current on this element peaks at negative scan angle, but the focal plane feed has a much narrower dependence on scan angle, and plays a role for scan around -45° .

Figure 12 shows the current on feed elements for an array with uniform illumination and scanned to broadside using a time delay feed. Figure 12A shows the current using the feed in the focal plane ($h=0$), and though broadside is not one of the critical angles, still most of the power is constrained to two elements. Figures 12B and C show amplitude and phase for the array with the feed moved to a point closer to the lens by 4 wavelengths ($h=-4\lambda$) than the focal point feed of 12A. This current is spread out among many more elements. 12C shows the phase controlling the diverging field on transmit.

Figure 13 is similar to 12, but for the uniformly illuminated array scanned to 57° ($u_0=0.8379$), one of the critical angles. The figure compares the data of Figure 6B for the time delayed focal point feed, and again shows that more feed elements share the power.

Figure 14 illustrates that for most of these scan angles, at least 5 feed elements out of 16 carry significant power. This is a substantial improvement over the 1 or 2 elements with the focal plane feed.

Figure 15 shows a subset of element currents for the focal plane and displaced feeds, in this case for an input weighting that corresponds to a low sidelobe Taylor taper of -40 dB. Again the focal plane feed has significant current on only two elements at a time, while there is far more overlap for the off axis synthesized beamformer.

Figure 16 shows the number of elements with significant power for the focal plane feed and the displaced feed with a synthesized beamformer. For the focal plane feed only one or two of the 16 feed elements are used, while the displaced feed uses four or five elements except at large scan angles. This advantage is not as large as for the transmit case, but still significant.

Figure 17 shows typical radiation patterns for the array of 256 elements grouped into 16 subarrays for insertion of time delay and amplitude weighting. A -40 dB Taylor taper was chosen, and the network yielded near-sidelobes between -25 dB and -30 dB over the bandwidth. These sidelobe levels are essentially the same as for the focal plane feed (data not shown), so the only compromise is a small loss in bandwidth. The computed 5 % bandwidth corresponds to about a factor of 5 bandwidth increase relative to the array without time delays.

5. Summary and Conclusions:

This paper has presented results of displacing the feed of a dual-transform wideband scanning systems in order to avoid the dynamic range problems associated with a focal plane feed. The focal plane feed is shown to never use more than two elements out of the 16 feed elements, while the synthesized feed illumination uses at least four or five of the feed elements while producing good subarray patterns and radiation patterns.

A future task is to examine the mutual coupling conditions for the feed elements operating in the converging or diverging field area.

6. Acknowledgement

The author is grateful to the Air Force Office of Scientific Research for sponsoring this work, to Dr. Joseph Teti of Emergent Information Technologies

Inc., and Dr. Mark Mitchell of Georgia Tech. Research Institute who first introduced me to this problem and its consequences.

7. References

- [1] R. Tang, "Survey of Time-Delay Steering Techniques," Phased Array Antennas, pp. 254-260, Artech House, Dedham, MA, 1972
- [2] R. J. Mailloux, "Special Array Feeds for Limited Field-of-View and Wide-Band Arrays," Chapter 8 in Phased Array Antenna Handbook, pp 511-521, Artech House Inc, 1994
- [3] R. Tang and R.W. Burns, "Phased Arrays," Ch 20 in Antenna Engineering Handbook, pp. 20-51, R.C. Johnson, Editor, Third Edition 1993
- [4] R. L. Fante, " Systems Study of Overlapped Subarrayed Scanning Antennas", IEEE Trans. Vol. AP-28, No.5, pp. 668-679, Sept 1980
- [5] H. L. Southall, D.T. McGrath, " An Experimental Completely Overlapped Subarray Antenna", IEEE Trans. Vol. AP-34, No. 4, pp. 465-474, April 1986

Figure 1: Subarrays for Large Wide-Band Arrays

Subarrays reduce the number of time delays

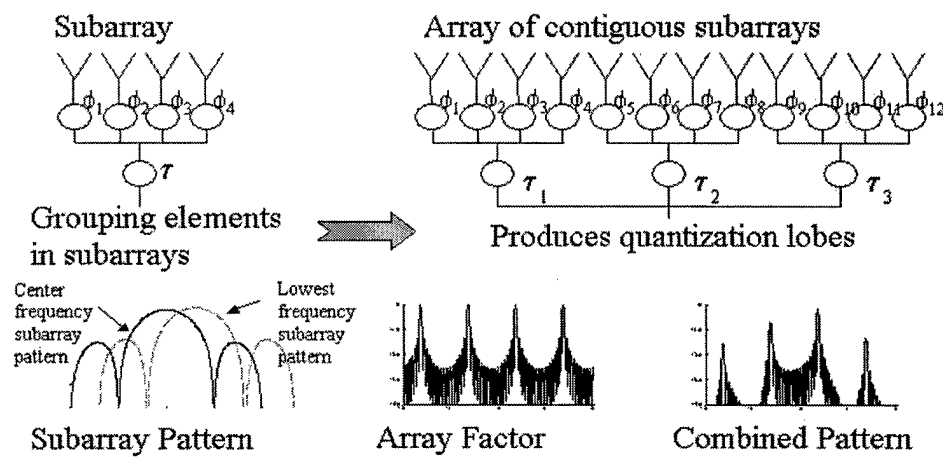


Figure 2: Pattern of 256 element array with 8 tapered subarray weights

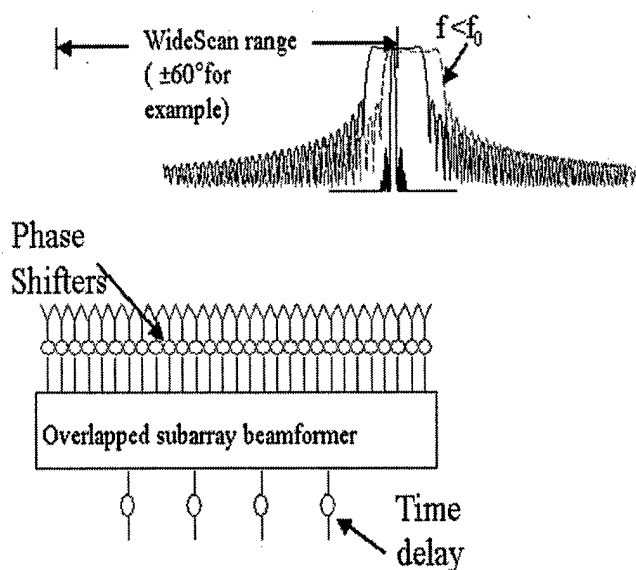
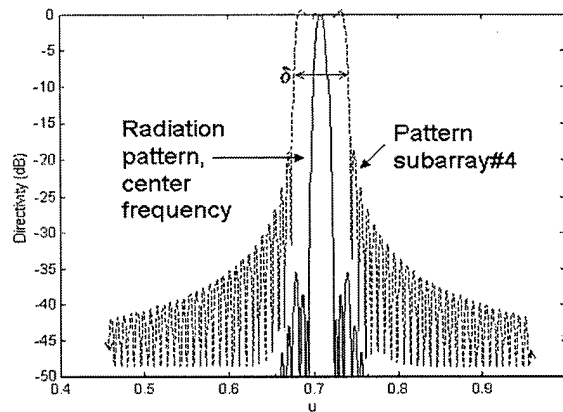


Figure 3: Overlapped subarrays to reduce the number of time delays in large arrays at wide scan angles

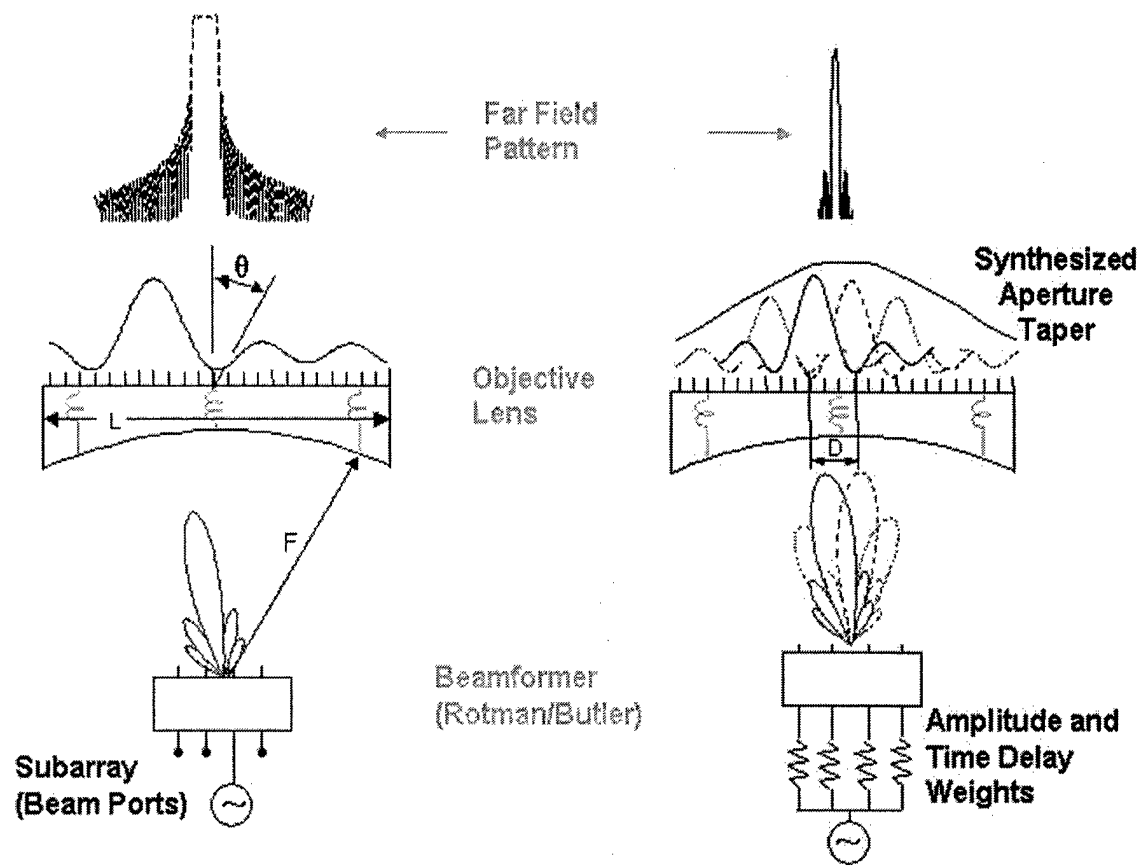
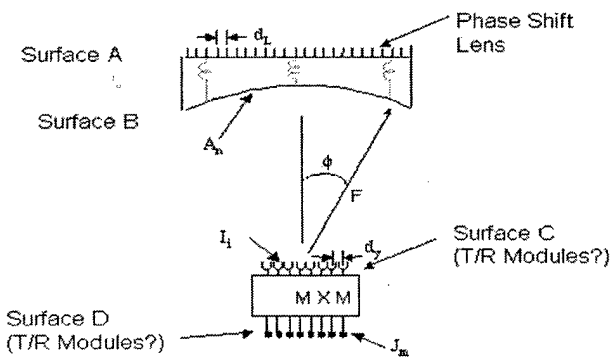


Figure 4:Overlapped Subarrays for Wideband Scanning

- High loss architecture, 6 dB or more.
Where to put amplification ?



T/R modules (amplification) at surface C seems ideal !

Figure 5

Normalized Current on Feed Elements

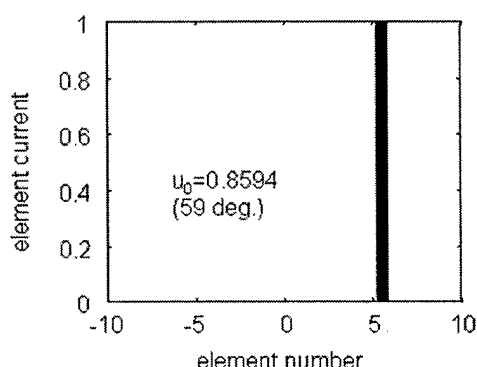


Fig 6A 16 Element
Orthogonal Feed

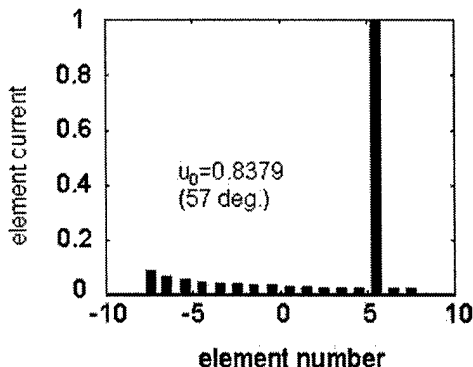


Fig 6B 16 Element
Time Delayed Feed

Figure 6: Normalized Current on Elements at Critical Angles with Focal Plane Beamformer ($h_i = 0$) for Uniformly Illuminated Array at $f = 0.975 f_0$

Current on Elements

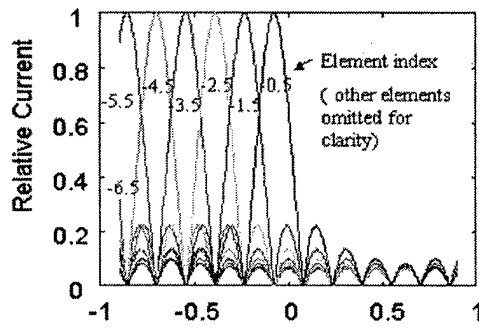


Fig 7A 16 Element
Orthogonal Feed

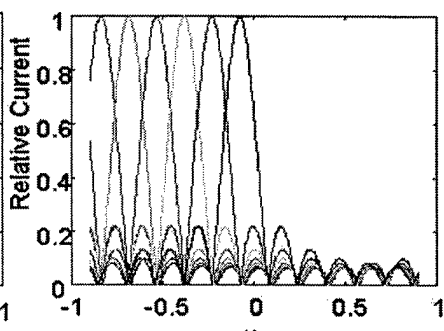


Fig 7B 16 Element
Time Delayed Feed

Figure 7: Normalized Current Amplitude on Elements at $f = .975 f_0$ and with Focal Plane Beamformer ($h = 0$) for Uniformly Illuminated Array

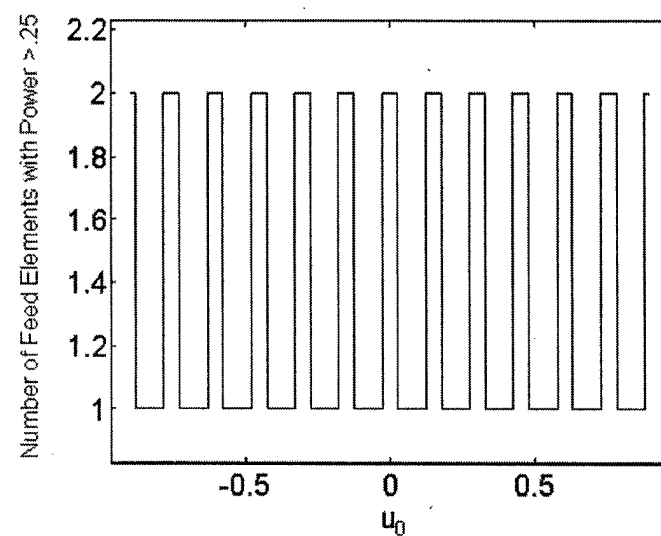


Figure 7C: Number of Elements with Normalized Power > 0.25 of Maximum Element Power (time delayed feed at focal plane)

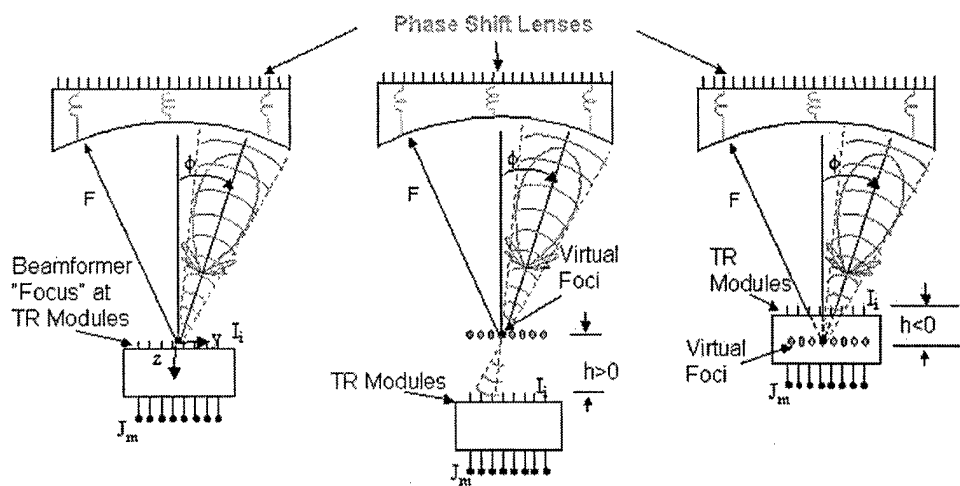
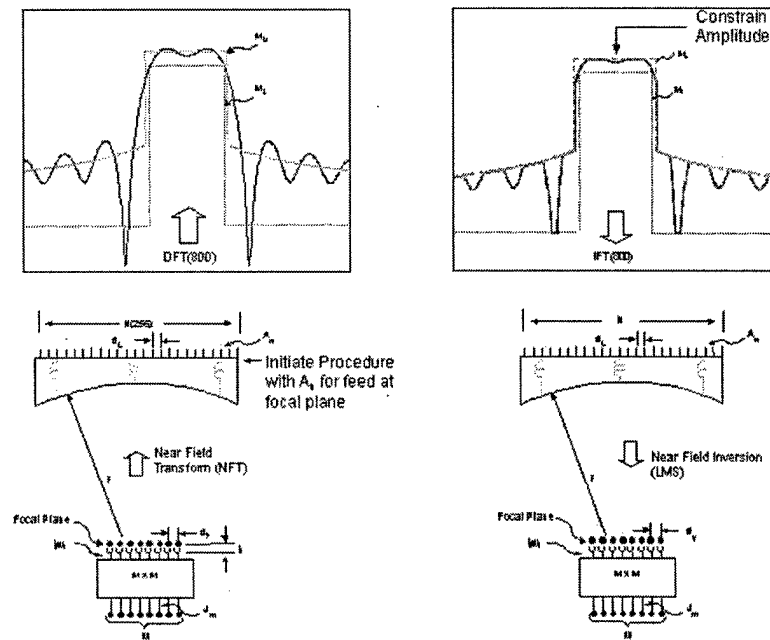


Figure 8: Alternative Subarray Beamformer Configurations

Figure 9: Alternating Projection Method Used to Optimize Subarray Patterns for Feed Beyond Focal Plane



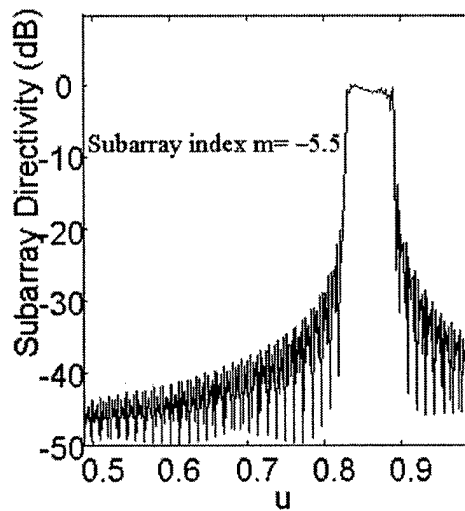


Figure 10A: focal plane beamformer

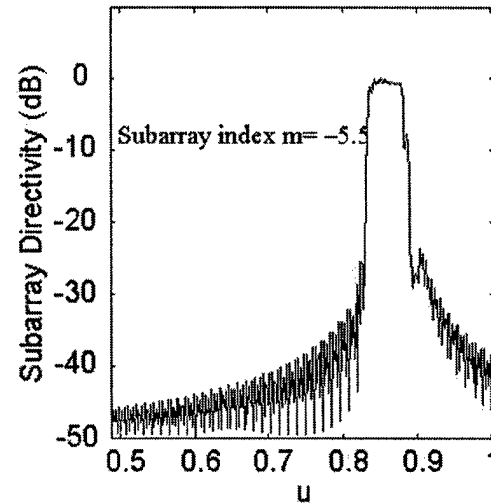


Figure 10B: synthesized beamformer

Figure 10: Subarray Patterns for $u_0 = 0.8594$ Using Focal Plane and Synthesized Beamformer

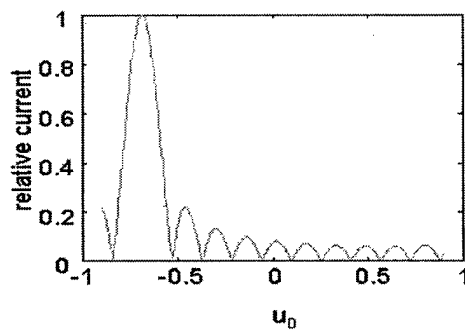


Fig11A: Focal Plane Beamformer ($h=0$)

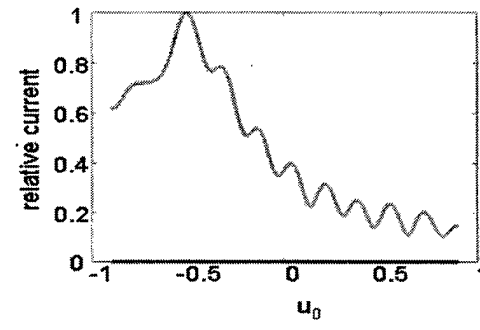


Fig11B: Synthesized Beamformer ($h = -4$)

Figure 11: Current on element number -5.5 for $|u| < 0.9$ using time delayed feed

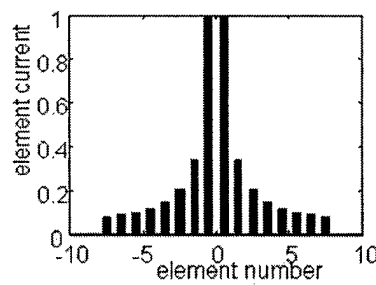


Fig12A: Focal Plane Beamformer

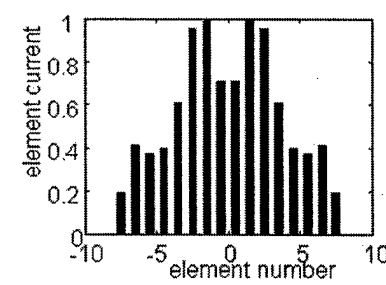


Fig12B: Synthesized Beamformer ($h = -4$)

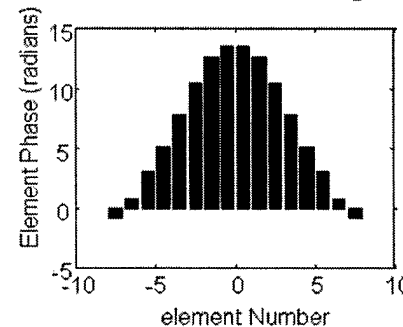


Fig12C: Phase of Current
for Synthesized Beamformer
($h = -4$)

Figure 12: Normalized Amplitude and Phase of Current on Feed
Elements of Uniformly Illuminated Array at Broadside

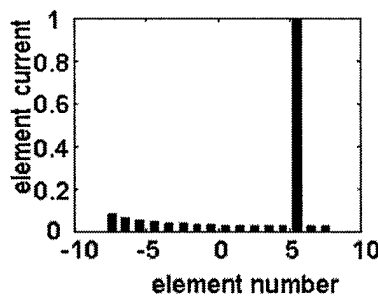


Fig13A: Focal Plane Beamformer

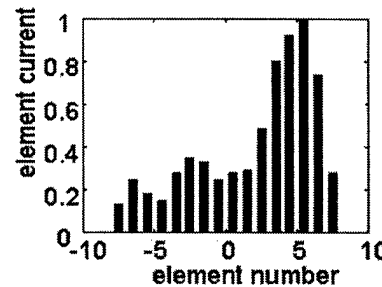


Fig13B: Synthesized Beamformer ($h = -4$)

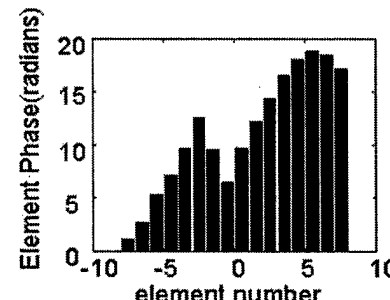


Fig13C: Phase of Current
for Synthesized Beamformer
($h = -4$)

Figure 13: Normalized Amplitude and Phase of Current on Feed

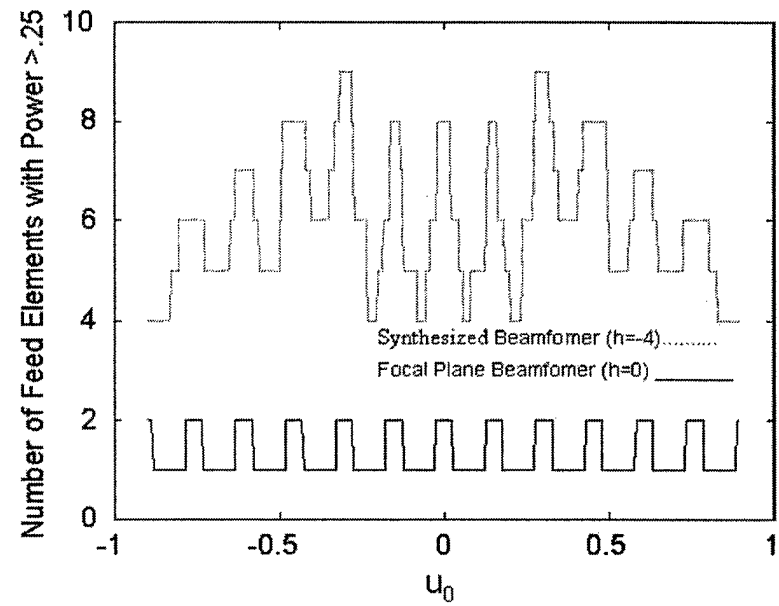


Figure 14: Number of Elements with Normalized Power > 0.25 of Maximum Element Power for Array at Broadside and Uniform Illumination using a 16 element time delay beamformer

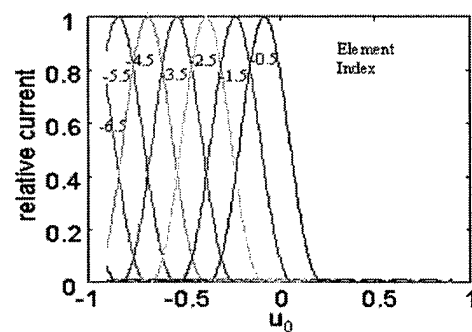


Fig 15A:Focal Plane Feed

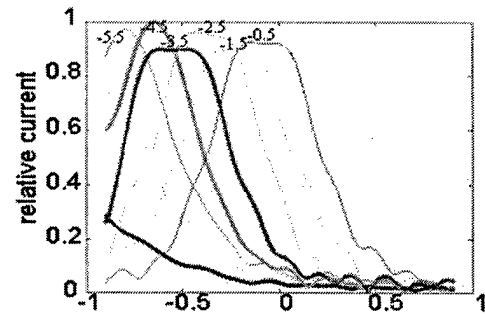


Fig 15B: Displaced Synthesized Feed

Figure 15: Current Amplitude on Elements with Focal Plane Feed ($h = 0$) and Displaced Beamformer ($h = -4$)

(low sidelobe case)

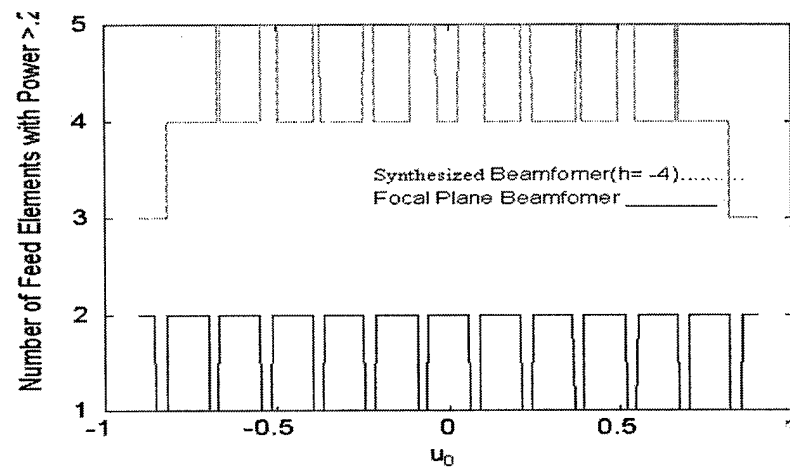


Figure 16: Number of Feed Elements with Normalized Power > 0.25 of Maximum Element Power for Low Sidelobe Array

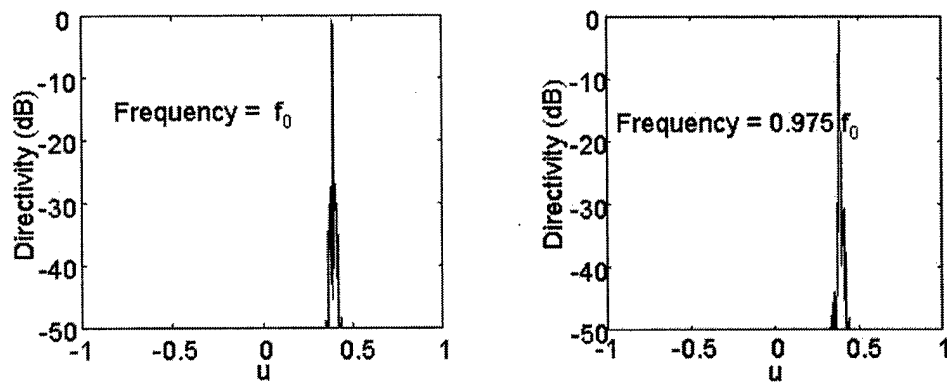


Fig17A

Fig17B

Figure 17: Radiated Patterns from Array using Displaced Feed with Synthesized Beamformer

AD NUMBER	DATE	DTIC ACCESSION NOTICE
1. REPORT IDENTIFYING INFORMATION		REQUESTER
A. ORIGINATING AGENCY		1. Put your name and address on reverse side of this form
AFRL/SNH		2. Complete in block form
B. REPORT TITLE AND/PR NUMBER		3. Attach five copies of this form
See Attached List		mailed
C. MONITOR REPORT NUMBER		4. Use unique identifier informally
N/A		5. Do not use for 6 to 8 weeks
D. PREPARED UNDER CONTRACT NUMBER		
N/A		
2. DISTRIBUTION STATEMENT		
A. Cleared for Public Release		
DTIC:		
		1. Assign AD Number 2. Return to monitor

DTIC Form 30
JUL 95

PREVIOUS EDITIONS ARE OBSOLETE